

Synthesis and Characterization of New Pyrrolidinium Based Protic Ionic Liquids. Good and Superionic Liquids

Mérièm Anouti,^{*,†} Magaly Caillon-Caravanier,[†] Yosra Dridi,[†] Herve Galiano,[‡] and Daniel Lemordant[†]

Laboratoire PCMB (EA 4244), Équipe de Chimie-physique des Interfaces et des Milieux Electrolytiques (CIME), Université François Rabelais, Parc de Grandmont 37200 Tours, France, and CEA, LE RIPAUT, Laboratoire Synthèse et Transformation des Polymères, CEA, F-37260 Monts, France

Received: July 7, 2008; Revised Manuscript Received: August 11, 2008

New pyrrolidinium-cation-based protic acid ionic liquids (PILs) were prepared through a simple and atom-economic neutralization reactions between pyrrolidine and Brønsted acids, HX, where X is NO₃[−], HSO₄[−], HCOO[−], CH₃COO[−] or CF₃COO[−] and CH₃(CH₂)₆COO[−]. The thermal properties, densities, electrochemical windows, temperature dependency of dynamic viscosity and ionic conductivity were measured for these PILs. All protonated pyrrolidinium salts studied here were liquid at room temperature and possess a high ionic conductivity (up to 56 mS cm^{−1}) at room temperature. Pyrrolidinium based PILs have a relatively low cost, a low toxicity and exhibit a large electrochemical window as compared to other protic ionic liquids (up 3 V). Obtained results allow us to classify them according to a classical Walden diagram and to determinate their “Fragility”. Pyrrolidinium based PILs are good or superionic liquids and shows extremely fragility. They have wide applicable perspectives for fuel cell devices, thermal transfer fluids, and acid-catalyzed reaction media as replacements of conventional inorganic acids.

1. Introduction

Ionic liquids (ILs) are class of chemicals composed entirely of ions with melting points below 100 °C. Due to their unique physicochemical properties, they have rapidly gain in interest as greener replacements of traditional volatile organic solvents (VOCs). Other main benefits of ionic liquids are their large liquid state range, favorable solvation behavior, low melting temperature, stability in air, high ionic conductivity and low vapor pressure. Modification of selectivity in chemical reactions, open new possibilities in various industrial fields such as catalysis, separation techniques, and electrochemical devices applications.

ILs can be used as safe and stable electrolyte in a variety of electrochemical devices, including electrochemical capacitors, high energy density batteries, solar cells and electrochromic windows.^{1–4} These ILs usually consist of an inorganic or organic anion and a nitrogen-containing organic cation such as alkylammonium, *N,N*-dialkylimidazolium, *N,N*-dialkylpyrrolidinium and *N*-alkylpyridinium,^{5–8} whereas the most commonly used ionic liquid anions include halide ions, tetrachloroaluminate (AlCl₄[−]), tetrafluoroborate (BF₄[−]), hexafluorophosphate (PF₆[−]), and bis[(trifluoromethyl)sulfonyl]imide anion (CF₃SO₂)₂N[−] (also known as bistriflylimide (Tf₂N[−])).^{1,6,9,10}

Room temperature ionic liquids (RTILs) are ILs that are liquid at room temperature or slightly higher (20–30 °C). Those formed by the transfer of a protons between a Brønsted acid and a Brønsted bases, form a protic subgroup in the class of ambient temperature fluid systems now referred as “Protic Ionic Liquids (PILs)”. Proton conducting electrolyte are now emerging as useful material owing to various possible applications such

as electrolyte in aqueous batteries, fuel cells, double layer capacitors, dye-sensitized solar cell, or actuators.^{11–21} These promise large new fields of application for PILs.

Over the past decade, chloroaluminate ionic liquids have gained increasing attention in replacement of the conventional mineral and solid acid catalysts.²² Nevertheless, chloroaluminate ionic liquids are very sensitive to hydrolysis.^{23,24} Trace amounts of water can change the composition of the salt and the concentration in protons. As a result, it is difficult to accurately control the acidity of these ionic liquids. ILs prepared from protonated imidazole and bis(trifluoromethanesulfonyl)amide could be used as nonaqueous proton-conducting electrolytes in fuel cell devices. However, the main disadvantages of imidazolium-based ILs are their relatively high cost and toxicity. Therefore, the development of water- and air-stable of low cost and low toxicity room temperature ILs is highly desirable.

We report in the present work the preparation of new pyrrolidinium based PILs containing NO₃[−], HSO₄[−], HCOO[−], CH₃COO[−], CF₃COO[−] or C₇H₁₅COO[−] anions obtained by neutralization of pyrrolidine by the corresponding Brønsted acid. Physicochemical properties of these PILs are determined and discussed according to the nature of the anion. The temperature dependency of the dynamic viscosity, ionic conductivity, and the phase behavior of these PILs have been measured and investigated in details. Results allow us to classify them according to a classical Walden diagram permit to evaluate their great ionicity. Finally their acidity scale are estimated from determination of Hammett's acidity function *H*₀, using UV–visible spectroscopy.

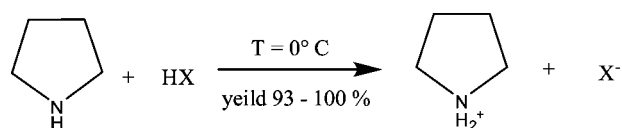
2. Experimental Section

2.1. Materials. Pyrrolidine and all organic acids are commercially available from Fluka (>99.0%) and are used without further purification. The nitric acid (68% in water) and hydro-sulfuric acid (96% in water) solution are obtained from Sigma

* Correspondance Author E-mail: meriem.anouti@univ-tours.fr. Fax: (33)247367360. Tel: (33)247366951.

[†] Université François Rabelais.

[‡] CEA.

SCHEME 1: Preparation of Pyrrolidinium Based Ionic Liquids

TABLE 1: Name, Structure and Abbreviation of Selected PILs

Ionic Liquid	Structure	Abbreviation
pyrrolidinium nitrate		[Pyr][NO ₃]
pyrrolidinium hydrogen sulfate		[Pyr][HSO ₄]
pyrrolidinium formate		[Pyr][HCOO]
pyrrolidinium acetate		[Pyr][CH ₃ COO]
pyrrolidinium trifluoroacetate		[Pyr][CF ₃ COO]
pyrrolidinium octanoate		[pyr][C ₇ H ₁₅ COO]

Aldrich. Water is purified with Milli-Q 18,3 MΩ water system and 1,2-dichloroethane DCE (>99,0%) is purchased from Sigma Aldrich.

2.2. Preparation of PILs. The preparation of alkyl ammonium-based ILs is illustrated in Scheme 1.

The nature of the X[−] anion is reported in the Table 1 with name, structure and abbreviation of the obtained PILs.

Preparation of Pyrrolidinium Based PILs with Organic Counteranion. The example of [Pyr][HCOO] shows a typical preparation method and a similar procedure is used with compounds [Pyr][CH₃COO], [Pyr][CF₃COO] and [pyrro][C₇H₁₅COO]. Pyrrolidine (38.55 g; 0.85 mol) is placed in a three-neck round-bottom flask immersed in an ice bath and equipped with a reflux condenser, a dropping funnel to add the acid and a thermometer to monitor the temperature. Under vigorous stirring, formic acid (61.45 g; 0.85 mol) is added dropwise to the pyrrolidine (60 min). As this acid–base reaction is strongly exothermic, the mixture temperature is maintained less than 25 °C during the addition of the acid by use of the ice bath. Stirring is maintained for 4 h at ambient temperature, a low-viscous liquid is obtained. This new phase is yellow pale-colored. The residual pyrrolidine or acid is evaporated under reduced pressure and the remaining liquid is further dried at 80 °C under reduced pressure (1–5 mmHg) to obtain the target IL (98.72 g; yield 98.7%). Neither crystallization nor solidification was observed on the liquid, stored for several weeks at 20 °C.

Preparation of Pyrrolidinium Based PILs with Inorganic Counteranion. [Pyr][NO₃] and [Pyr][HSO₄[−]] were obtained using the same procedure. We report only the preparation of

[Pyr][NO₃]. Pyrrolidine (26.78 g; 0.37 mol) is introduced in a two-necked round-bottom flask immersed in an ice bath and equipped with a dropping funnel to add nitric acid (68% in water) and a thermometer to control the temperature. Under vigorous stirring, nitric acid (34.54 g; 0.37 mol) is added dropwise to the flask in about 60 min (mixture temperature <35 °C). Stirring is maintained for 4 h at ambient temperature before adding 120 mL of DCE. Then, this mixture is distilled under normal pressure until the water–DCE a heteroazeotropic boiling point is reached (73 °C) to get rid of residual water. DCE is finally evaporated from the mixture under reduced pressure so that a pale yellow and viscous liquid can be collected (yield 93%).

2.3. Measurements. ¹H NMR spectrum are obtained using a Bruker 200 MHz spectrometer, CDCl₃ as solvent and TMS as internal standard.

Densities are determined by the weight method at 25 °C. Measurements of refractive index are realized at 25 °C with an ABBE refractive index instrument, calibrated with deionized water. Viscosities are measured using a TA instrument rheometer (AR 1000) with conical geometry at various temperatures (from 25 to 80 °C). Ionic conductivities are measured using a Crison (GLP 31) digital multifrequencies conductimeter. The temperature control (from 20 to 120 °C) is ensured by a JULABO thermostatted bath. PILs' electrochemical windows are checked by linear voltammetry at ambient temperature using an EGG M 270A Electrochemical Work Station and a three-electrodes configuration. A 3-mm-diameter carbon disk is used as a working electrode, a platinum wire as a counter electrode and an Ag/AgCl_{sat}, KCl_{sat}(PIL) electrode as reference. The reference Ag/AgCl_{sat}, KCl_{sat}(PIL) system is calibrated versus the SHE electrode using the ferrocenium ion/ ferrocene couple: $E_{ref} = 0.216$ mV/SHE.

The determination of the PILs Brønsted acidity scale is conducted on a Perkin-Elmer instrument Lambda 25 UV visible spectrophotometer with appropriate acido-basic indicators.

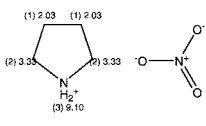
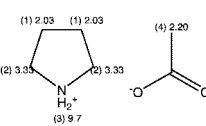
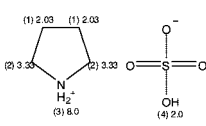
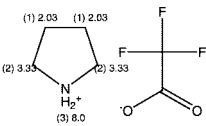
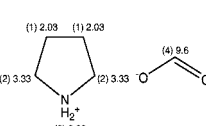
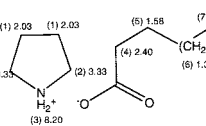
Differential scanning calorimetry (DSC) is carried out on a Perkin-Elmer DSC6 under a N₂ atmosphere. Samples for DSC measurements are sealed in Al pans. Thermograms are recorded during cooling (from +10 to −120 °C) at a scan rate of 5 °C min^{−1} and heating (from 10 to 400 °C) with a scan rate of 10 °C min^{−1}.

3. Results and Characterizations

3.1. ¹H NMR. Characteristic of ¹H NMR spectrums (200 MHz, CDCl₃, TMS) of PILs are resumed in Table 2. When D₂O is added, the signal due to the hydrogen carried by the nitrogen is the only one to disappear.

3.2. Physical Properties of PILs. Density. Density of ionic liquids falls typically in the range 1.2–1.6 g cm^{−3}.²⁵ However, those based on the dicyanoamide anion, [N(CN)₂][−],²⁶ for example exhibit a density lower than 1 g cm^{−3}. In general, densities of aprotic ionic liquids as alkylimidazolium are very strongly affected by the nature of the anion. For example, the densities of 1-butyl-3-methylimidazolium are equal to 1.2023, 1.3673, 1.2170 and 1.4366 g cm^{−3} for respectively BF₄[−], PF₆[−], TFA[−] and Tf₂N[−].²⁷ In this study, pyrrolidinium salts having a mineral counteranion have a larger densities than those having an organic anion: 1.1675 g cm^{−3} ([Pyr][NO₃]) and 1.3421 g cm^{−3} ([Pyr][HSO₄]) as compared to 0.9485, 1.0543 and 1.1190 g cm^{−3} for [Pyr][C₇H₁₅COO], [Pyr][CH₃COO] and [Pyr][HCOO], respectively. The pyrrolidinium trifluoroacetate has nevertheless a higher density, $\rho = 1.2310$ g cm^{−3}. Molecular packing in the liquid phase is enhanced when the substituent R in RCOO[−] is electron acceptor as the CF₃ group.

TABLE 2: ¹H-NMR Spectrum Characteristics of the PILs

PILs, δ in ppm	Characteristics	PILs, δ in ppm	Characteristics
	(1) q, 4H (2) t, 4H (3) s, 2H		(1) q, 4H (2) t, 4H (3) s, 2H (4) s, 3H
	(1) bs*, 4H (2) t, 4H (3) s, 2H (4) b.s., 1H		(1) bs*, 4H (2) t, 4H (3) s, 2H
	(1) q, 4H (2) t, 4H (3) s, 2H (4) s, 1H		(1) bs*, 4H (2) t, 4H (3) s, 2H (4) t, 2H (5)-(6) bs*, 10H (7) t, 3H

* b.s.: broad signal

TABLE 3: Molar Mass, Density, Molar Volume, Viscosity, Specific and Equivalent Ionic Conductivity of PILs at 25 °C and Effective Volume of Anions

ionic liquids	M (cm ³ mol ⁻¹)	ρ (g cm ⁻³) ± 0.1%	V_m (cm ³ mol ⁻¹) ± 0.1%	V^* (cm ³ mol ⁻¹)	η (mPa s) ± 0.1%	σ (mS cm ⁻¹) ± 2%	Λ (S cm ² mol ⁻¹) ± 2%
[Pyr][NO ₃]	134.13	1.1675	114.88	40.2	5.2	50.1	5.75
[Pyr][HSO ₄]	169.20	1.3421	126.07	51.4	190.1	6.8	0.86
[Pyr][HCOO]	117.08	1.1190	104.63	30	2.5	32.9	3.44
[Pyr][CH ₃ COO]	131.20	1.0543	124.44	49.7	30.2	5.9	0.73
[Pyr][CF ₃ COO]	185.14	1.2310	150.40	75.7	21.0	16.4	2.46
[pyrr][C ₇ H ₁₅ COO]	215.30	0.9485	226.99	152.3	36.5	0.8	0.18

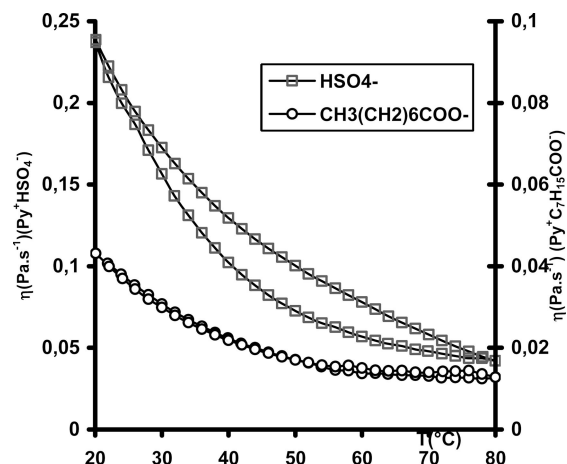
Viscosity. The viscosity of an ionic liquid is a very important parameter in electrochemical studies due to its strong effect on the rate of mass transport within solution. Generally, ionic liquids are more viscous than common molecular solvents ($\eta(\text{H}_2\text{O}) = 0.8903 \text{ mPa s}$ at 25 °C). Indeed, their viscosities typically range from 30 cP to about 100 cP at room temperature, but in some cases, values as high as 500–600 cP are observed.²⁸ The identities of the anion and the cation that compose the ionic liquid have a huge effect on the viscosity of the ionic liquid. With respect to the anionic species, higher basicity, size, and relative capacity to form hydrogen bonds result in more viscous ILs. Thus, protic ionic liquids containing PF₆[−] anions are much more viscous (1-ethyl-2-methylimidazolium PF₆[−],²⁹ $\eta > 1000 \text{ cP}$) than those formed with TFSI anions (1-ethyl-2-methylimidazolium TFSI,²⁹ $\eta = 69 \text{ cP}$), where the negative charge is more delocalized. Moreover, the viscosities of ionic liquids appear to be ruled also by van der Waals interactions,³⁰ and cationic size.³¹ The viscosities at 25 °C of synthesized [Pyr][HCOO] and the [Pyr][NO₃] DIPMF PILs are only 2.5 and 5.2 cP, respectively. These values are comparable to those measured for *N*-methylpyrrolidinium formate and *N*-methylpyrrolidinium acetate: 7.5 and 3.2 cP, respectively. The association of pyrrolidinium cation with HSO₄[−] anion leads more viscous salt, 190 cP. The van der Waals interactions are principal responsible for the higher viscosity of [Pyr][HSO₄] in comparison with [Pyr][HCOO], this is probably due to the more delocalized charge in HCOO[−] comparably to HSO₄[−].

Figure 1 exhibits the temperature dependence of viscosity data for [Pyr][HSO₄] and [Pyr][C₇H₁₅COO]. PILs viscosities exhibit typically non-Arrhenius behavior, i.e., a distinct down-

ward curvature at lower temperatures in the Arrhenius plot (Figure 2). Viscosity data can be fitted to the Vogel–Tamman–Fulcher (VTF) equation.

$$\eta = \eta_0 \exp\left[\frac{B}{(T - T_0)}\right] \quad (1)$$

where η_0 (Pa s^{−1}), B (K), and T_0 (K) are fitting parameters. As an example, in Figure 3 are plotted the variation of $\ln(\eta)$ versus $1/(T - T_0)$ for [pyrro][HSO₄]. The product BR (R is molar gas constant) has dimension of an activate energy (kJ mol^{−1}). The

Figure 1. Temperature dependence of viscosity data for [Pyr][HSO₄] and [Pyr][CH₃(CH₂)₆COO].

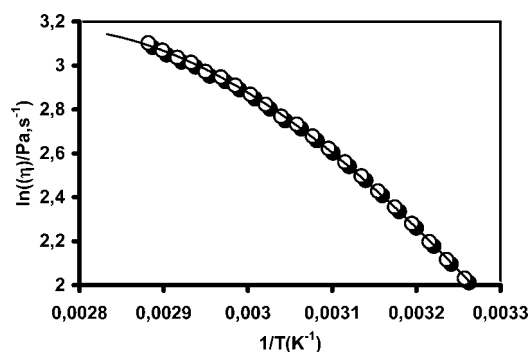


Figure 2. Arrhenius plot for the viscosity of pyrrolydinium hydrogen sulfate.

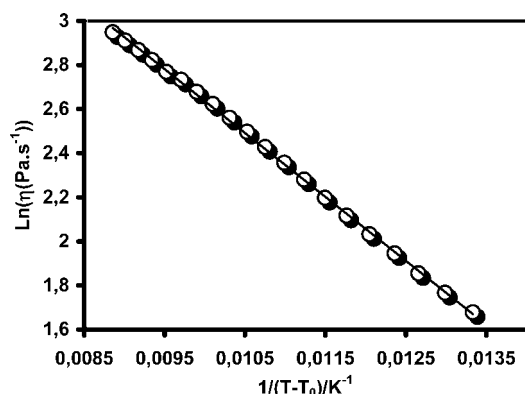


Figure 3. VTF plot of ionic conductivities and viscosities for pyrrolydinium hydrogen sulfate.

TABLE 4: VTF Equation Parameters for Viscosity (η_0 , B , T_0) (Eq 1)

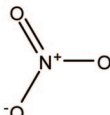
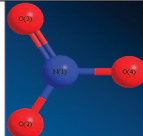
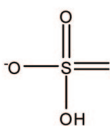
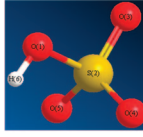
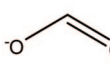
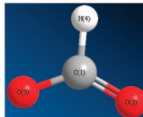
ionic liquids	η_0 (mP s)	T_0 (K)	B (K) ^a	R^{2b}
[Pyr][NO ₃]	1.7	208	102	0.9971
[Pyr][HSO ₄]	0.5	166	781	0.9970
[Pyr][HCOO]	0.3	177	247	0.9970
[Pyr][CH ₃ COO]	0.2	165	627	0.9998
[Pyr][CF ₃ COO]	1.5	214	222	0.9973
[Pyr][CH ₃ (CH ₂) ₆ COO]	0.3	167	616	0.9995

^a BR \equiv activation energy (kJ mol⁻¹). ^b Correlation coefficient.

best-fit η_0 (cP), B (K), and T_0 (K) parameters are given in Table 4.

Conductivity. Ionic conductivity is one of the most important properties of ILs considered as electrolytes. Ionic liquids have reasonably good ionic conductivities compared to those of organic solvents/electrolyte systems (up to 10 mS cm⁻¹).³² However, at room temperature, their conductivities are usually lower than those of concentrated aqueous electrolytes, based on the fact that ionic liquids are composed exclusively of ions. PILs conductivities are higher than those of aprotic ILs.²⁸ The conductivity at 25 °C of the six PILs under study falls between 0.8 and 50.1 mS cm⁻¹ (Table 2). These values are comparable to the most conductive PILs among salts based on alkylammonium (methylammonium formate, σ = 43.8 mS cm⁻¹;³³ ethylammonium nitrate, σ = 39.6 mS cm⁻¹;³⁴ imidazolium (1-methylimidazolium formate, σ = 20 mS cm⁻¹;³⁵ 1-methylimidazolium HSO₄, σ = 6.5 mS cm⁻¹;³⁶ pyrrolidinium (pyrrolidinium TFSA, σ = 39.6 mS cm⁻¹;³⁷ *N*-methylpyrrolidinium acetate, σ = 2 mS cm⁻¹;³⁵). It is found in this study that the conductivity of nitrate and formate anion-based PILs, σ = 50.1 and 32.9 mS cm⁻¹, respectively, are higher than the four other anion-based PILs {[Pyr][HSO₄]⁻, 6.8; [Pyr][CH₃COO]⁻, 5.9

TABLE 5: 3D Representation and Mulliken Charges^a Calculated with GAMESS Interface

Anion	3D representation of anion	Mulliken charges calculated with Gamess interface
		N(1) : 0.636733 O(2) : -0.545336 O(3) : -0.546064 O(4) : -0.545333
		O(1) : -0.813020 S(2) : 1.942342 O(3) : -0.820603 O(4) : -0.847191 O(5) : -0.843858 H(6) : 0.382330
		C(1) : 0.615851 O(2) : -0.789821 O(3) : -0.789658 H(4) : -0.036372

^a Calculation method RHF/3-21G (restricted Hartree-Fock, basic set 3-21G), GAMESS interface.

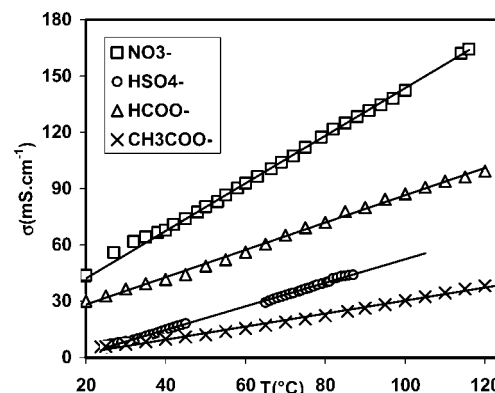


Figure 4. Temperature dependence of ionic conductivity for four selected PILs.

mS cm⁻¹; [Pyr][CF₃COO]⁻, 16.4 mS cm⁻¹; [Pyr][C₇H₁₅COO]⁻, 0.8 mS cm⁻¹}, which correlates well to the difference in the anion size³⁸ and anion basicity. Large size anions lead to lower ion mobility which results in a lower conductivity.³⁹

The lower steric hindrance of the unsubstituted pyrrolidinium ring comparatively to alkylpyrrolidinium, is responsible for the high conductivity of the pyrrolidinium based PILs. Moreover, the presence of anions with localized charge (Table 5), above and below the pyrrolidinium ring, clearly restricts their mobility ring. This observation is also true for PILs based on imidazolium cation ([MeIm][HCOO], σ = 20 mS cm⁻¹;³⁵ [MeIm][CH₃COO], σ = 4 mS cm⁻¹;³⁵ [MeIm][HSO₄], σ = 6.5 mS cm⁻¹;³⁶).

Temperature dependency of ionic conductivity for four PILs is shown in Figure 4. As expected from the viscosity results, PILs conductivities exhibit non-Arrhenius behavior. Therefore, the Vogel–Tammann–Fulcher (VTF) equation was used to represent the temperature dependence of conductivity. As an example, in Figure 5 are plotted the variation of ln(σ) versus $1/(T - T_0)$ for [Pyr][NO₃]⁻, [Pyr][HSO₄]⁻, [Pyr][HCOO]⁻ and [Pyr][CH₃COO]⁻. The best-fit values for σ_0 (mS cm⁻¹), B' (K), and T_0 (K) parameters are given in Table 6.

Electrochemical Stability. Electrolytes for electrochemical devices should resist to reduction and oxidation and exhibit a

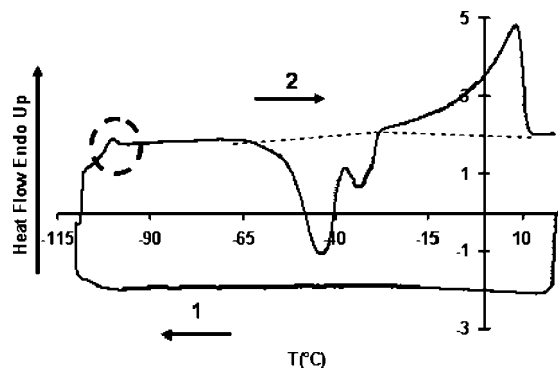


Figure 7. DSC thermogram of pyrrolidinium acetate.

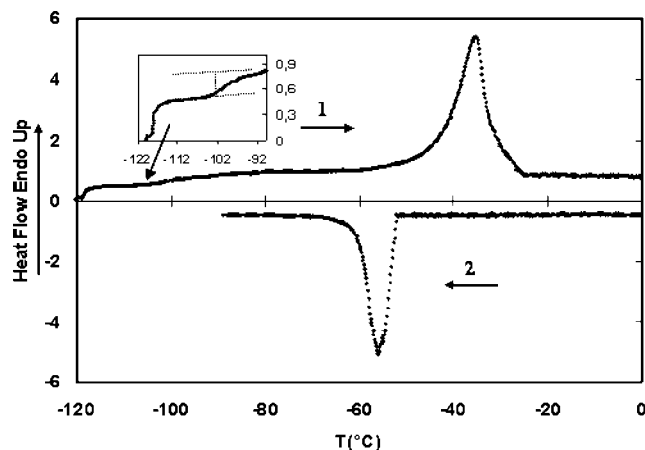


Figure 8. DSC thermograms of pyrrolidinium octanoate.

$\text{m}^{-3}) = 158$ to 206 for all PILs studied except for $[\text{Pyr}][\text{C}_7\text{H}_{15}\text{COO}]$ (D_h (MJ m^{-3}) = 45). All values are much higher than the minimum storage density (1.9 MJ m^{-3}) specified by the American National Renewable Energy Laboratory,⁴⁰ indicating that these PILs could be potentially used as excellent heat transfer fluids.

It is worthwhile to note that four PILs, $[\text{Pyr}][\text{NO}_3]$, $[\text{Pyr}][\text{HCOO}]$, $[\text{Pyr}][\text{CF}_3\text{COO}]$, and $[\text{Pyr}][\text{CH}_3(\text{CH}_2)_6\text{COO}]$ have freezing points on the cooling scan and melting point on the reverse scan, whereas two PILs $[\text{Pyr}][\text{CH}_3\text{COO}]$ and $[\text{Pyr}][\text{HSO}_4]$, exhibits no freezing point on cooling.

$[\text{Pyr}][\text{CH}_3\text{COO}]$ (Figure 7) and $[\text{Pyr}][\text{HSO}_4]$ exhibit on heating successively a glass transition, followed by a crystallization and fusion. On the cooling scan nonpeaks are detected which means that an amorphous phase is obtained. As an example, the DSC thermograms of $[\text{Pyr}][\text{CH}_3\text{COO}]$ are reported Figure 7. For pyrrolidinium octanoate (Figure 8), only a glass transition temperature was observed on heating scan after a “quenching” the sample by brutally immersing them in liquid nitrogen. Interestingly, $[\text{Pyr}][\text{CH}_3\text{COO}]$, exhibited two distinct exothermic transitions at -65 and -38 °C on the heating scan (Figure 7), which implied probably a solid–solid phase transition. $[\text{Pyr}][\text{NO}_3]$ ($T_{\text{fr}} = -27, 38$ °C) and $[\text{Pyr}][\text{CF}_3\text{COO}]$ ($T_{\text{fr}} = -48, -35$ °C) exhibit the same comportment. All pyrrolidinium PILs show substantial supercooling as the freezing points of the samples are significantly lower than the corresponding melting points (Table 8).

Ionic liquids can be thermally stable up to 450 °C. The thermal stability of ionic liquids is defined respectively by the strength of their heteroatom–carbon and heteroatom–hydrogen bonds. Wilkes et al. reported⁴¹ that the ILs 1-ethyl-3-methylimidazolium tetrafluoroborate, 1-butyl-3-methylimidazolium

tetrafluoroborate and 1,2-dimethyl-3-propylimidazolium bis-[(trifluoromethyl)sulfonyl]imide are stable respectively up to 445 , 423 , and 457 °C. In this study, early decomposition of all pyrrolidinium based PILs (130 °C $< T_d < 180$ °C) is probably due to a degradation reaction of the pyrrolidinium cation.

3.3. Ionicity and “Fragility” of Protic Ionic Liquids Studied. Ionicity. One way of assessing the ionicity of ionic liquids is to use the classification diagram based on the classical Walden rule.⁴² The Walden rule relates the ionic mobilities represented by the equivalent conductivity Λ to the fluidity η^{-1} of the medium through which the ions move. The equivalent conductivities Λ are calculated by use of the relation $\Lambda = V_e \sigma$, where V_e is the molar volume. Figure 9 shows variation of $\ln(\Lambda)$ versus $\ln(1/\eta)$ at various temperatures for four selected PILs. The ideal line is obtained on the basis that ions have mobilities that are determined only by the viscosity of the medium, and that the number of ions present in the equivalent volume is that indicated by salt composition; i.e., all ions contribute equally.⁴³ The position of the ideal line is established using aqueous KCl solutions at high dilution. The results obtained for selected PILs are plotted in Figure 9.

All PILs studied in this work are conforming to the Walden rule. Indeed, they lie significantly closer to the ideal line with unit slope than aprotic ILs like quaternary ammonium tetrafluoroborate.^{44–46} The Figure 9 also show that $[\text{Pyr}][\text{NO}_3]$ and $[\text{Pyr}][\text{HSO}_4]$ lie closely to the ideal line. $[\text{Pyr}][\text{NO}_3]$ and $[\text{Pyr}][\text{HSO}_4]$ lie in the upper part of the Walden diagram. This means they are superior conductors in which the Grothus mechanism for the transport of protons become predominant. Nitrate (NO_3^-) ions confer to ionic liquids a better ionic mobility and a greater fluidity as compared to formate (HCOO^-) and acetate (CH_3COO^-) ions. This is probably due to their size and their charge density. Such anions could serve as the proton transporting particles in high-temperature fuel cells.

Fragility. Fragility is a novel concept applicable to the study the behavior of glass-forming liquids. In a simplified picture, fragility is associated with the profile of the potential energy surface, and it increases with the mean amplitude and variance of the activation barriers. Several approaches have been made to quantify fragility in glassy state physics.^{47,48} A plot of $\ln(\eta)$ versus the scaled temperature T_g/T is more useful in visualizing comparative fragilities. Angell⁴⁹ has classified glass-forming liquids as “strong” and “fragile” on the basis of such a plot. Arrhenius liquids are described as strong while those following the VTF equation are fragile.

Fragility itself has been quantified in various ways.

(i) Fragility (F) as $F = 1/D$,⁴⁸ where D is an exponent parameter in the VTF equation written as

$$\eta = \eta_0 \exp \left[\frac{DT_0}{T - T_0} \right]$$

(ii) Fragility (F) as the ratio $F = T_0/T_g$,^{50,51} where T_0 and T_g are respectively “ideal” glass transition temperature (T_0) and glass transition temperature (T_g). This ratio conveniently lies between 0 (strong) and 1 (fragile).

(iii) Fragility $F_{1/2}$ (not F) is given by⁵²

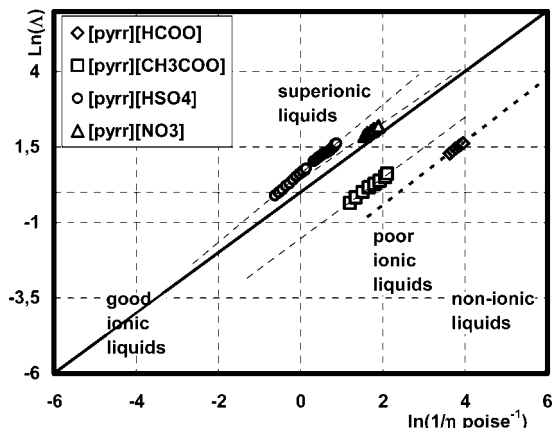
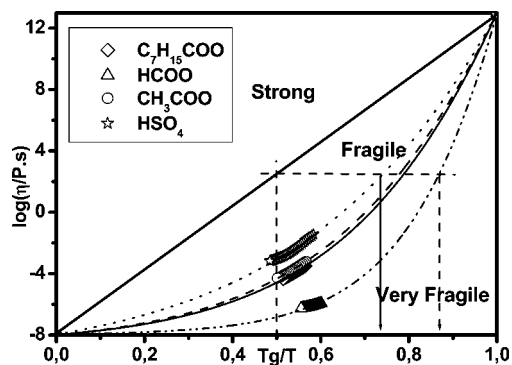
$$F_{\text{kin},1/2} = (T_g/T_{1/2})$$

where $T_{1/2}$ is the temperature at which $\log \eta$ is halfway the above range (see Figure 10). It is this last relation which we have adopted for fragility determination.

In Figure 10, we plot the data for a selection of four PILs. The fragility index parameters $F_{\text{kin},1/2}$ (relation in (iii)) are collected in Table 9. It can be seen that the $[\text{Pyr}][\text{HSO}_4]$,

TABLE 8: Thermal Properties of PILs [Melting Point (T_m), Freezing Point (T_{fr}), Decomposition Temperatures (T_d), Glass Transition (T_g) Temperatures, Specific Heat Capacity (C_p), and Energy Storage Densities (D_h)]

PILs	temperature/°C				$C_p/\text{J g}^{-1} \text{K}^{-1}$ (at 25 °C)	$D_h/\text{MJ mol}^{-39}$ ($\Delta T = 100$ °C)
	T_m	T_{fr}	T_g	T_d		
[Pyr][NO ₃]	−15	(−27, 38)	n.o	158	1.70	198
[Pyr][HSO ₄]	−30	−45	−102	130	1.54	206
[Pyr][HCOO]	−10	−60	−85	170	1.55	173
[Pyr][CH ₃ COO]	−5	(−65, −38)	−104	163	1.50	158
[Pyr][CF ₃ COO]	−10	(−48, −35)	n.o	180	2.25	276
[Pyr][C ₇ H ₁₅ COO]	−40	−53	−105	160	0.45	42

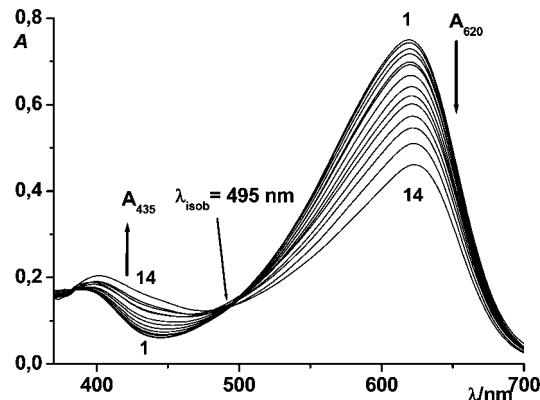
^a $D_h = \rho C_p \Delta T$.**Figure 9.** Walden plots for protic ionic liquids.**Figure 10.** Fragility plot for a selection of four PILs of this study.**TABLE 9: Glass Transition Temperature (T_g) and Fragility Parameters for PILs**

substance	T_g K)	$T_g/T_{1/2}$	$F_{kin,1/2}$
[Pyr][HSO ₄]	171	0.73	0.46
[Pyr][CH ₃ COO]	188	0.78	0.56
[Pyr][C ₇ H ₁₅ COO]	168	0.79	0.58
[Pyr][HCOO]	169	0.87	0.74
0.6 KNO ₃ , 0.4 Ca(NO ₃) ₂ ⁵³ (fragile)	340	0.82	0.64
GeO ₂ ⁵³ (strong)	810	0.55	0.24

[Pyr][CH₃COO], and [Pyr][C₇H₁₅COO] are very fragile compared to extremely fragile salts like mixture 0.6 KNO₃, 0.4 Ca(NO₃)₂.⁵³ [Pyr][HCOO] is extremely fragile.

Protonic ILs that have large hydrogen-bonding contributions to interparticle interactions will therefore tend to have the most extended intermediate range order.

3.4. Acidity Scale Determination. Determining a Brønsted acidity scale for ionic liquids aims at finding a correlation between their catalytic activities and their acidity for various acid–base reactions.⁵⁴ Proton acidity is mainly defined by their solvation. Indeed, faintly solvated protons show a higher

**Figure 11.** Absorption spectra of bromothymol blue for various concentrations of CH₃COOH in [Pyr][CH₃COO].

chemical activity. Protons properties in PILs depend on the strength of the acid providing the anion in its composition. Brønsted acidity of ILs has been estimated by Thomazeau et al.⁵⁵ from the determination of Hammett's acidity functions H_0 , using UV–visible spectroscopy.

In this work, various volumes of CH₃COOH are added to [pyrr][CH₃COO] (S solvent) containing bromothymol blue indicator whose $pK(I)_{aq} = 7.0$. As the acid concentration increases, a decreasing can be observed in the absorption band due to the basic form I^- at $\lambda = 620$ nm which is progressively replaced by of the protonated form HI at $\lambda = 435$ nm. The bundle of curves reported in Figure 11 show the displacement of the HI/I^- equilibrium when CH₃COOH is added. An isobestic point at $\lambda = 495$ nm indicates the that only two forms of the dye indicator are present in solution: $I^- + H^+ \rightleftharpoons HI$. The absorption at 620 nm is all along due to the two forms of the indicator: $A_{620} = \epsilon_{HI}^{620}l[HI] + \epsilon_{I^-}^{620}l[I^-]$, using C_I for the whole initial concentration: $C_I = [I^-] + [HI]$. A_{max}^{620} for the initial absorption at 620 nm is only due to the basic form $A_{max}^{620} = \epsilon_{I^-}^{620}lC_I$. A_{min}^{620} for the final absorption at 620 nm of the totally protonated indicator in presence of an acid excess is $A_{min}^{620} = \epsilon_{HI}^{620}lC_I$. The ratio $[I^-]_s/[HI]_s$ may be written as $[I^-]_s/[HI]_s = (A - A_{min})/(A_{max} - A)$.

TABLE 10: Calculation of the Hammett Function of CH₃COOH in [Pyr][CH₃COO]

$\log[\text{CH}_3\text{COOH}]/\text{mol L}^{-1}$	A_{620}	$(A_{max} - A)/(A - A_{min})$	$\log([I^-]/[HI])$	H_0 (± 0.05)
−0,3154	0,7131	0,1417	−0,8487	8,0487
−0,1946	0,6946	0,1774	−0,7512	7,9512
−0,1019	0,6733	0,2210	−0,6556	7,8556
−0,0407	0,6560	0,2589	−0,5868	7,7868
0,0302	0,6427	0,2898	−0,5380	7,738
0,0849	0,6178	0,3519	−0,4536	7,6536
0,1459	0,5957	0,4122	−0,3848	7,5848

Taking K_{HI} as the protonation equilibrium constant for the indicator: $K(\text{HI})_{\text{s}} = [\text{H}^+]_{\text{s}}[\text{I}^-]_{\text{s}}/[\text{HI}]_{\text{s}}$. The following relation may be established between $\text{p}K(\text{HI})_{\text{s}}$, H_0 , and the absorbencies

$$\text{p}K(\text{HI})_{\text{s}} = H_0 + \log[(A_{\text{max}} - A)/(A - A_{\text{min}})] \quad (4)$$

where H_0 is the Hammett's function defined as

$$H_0 = -\log a(\text{H}_{\text{aq}}^+) - \log\left(\frac{\gamma(\text{I}^-)}{\gamma(\text{HI})}\right) + \log\left(\frac{\Gamma(\text{I}^-)}{\Gamma(\text{HI})}\right) \quad (5)$$

In eq, $\gamma(\text{I}^-)$ and $\gamma(\text{HI})$ representing respectively the activity coefficients for the nonprotonated and the protonated form of the indicator $\Gamma(\text{I}^-)$ and $\Gamma(\text{HI})$ their transfer activity coefficients from an aqueous phase to the considered media.

At infinite dilution in the aqueous phase, H_0 is equal to the pH: $H_0 = -\log [\text{H}^+]$ and then $H_0 = \text{p}K_{\text{a}}(\text{CH}_3\text{COOH})_{\text{s}} + \log[\text{CH}_3\text{COO}^-] - \log[\text{CH}_3\text{COOH}]_{\text{aj}}$. So, eq can then be written as

$$\log\left(\frac{A_{\text{max}} - A}{A - A_{\text{min}}}\right) = \text{p}K(\text{HI})_{\text{s}} - \text{p}K_{\text{a}}(\text{CH}_3\text{COOH})_{\text{s}} + \log\left(\frac{[\text{CH}_3\text{COOH}]_{\text{aj}}}{[\text{CH}_3\text{COO}^-]}\right) \quad (6)$$

where $[\text{CH}_3\text{COO}^-]$ is the molarity of the ionic liquid, nearly constant during the acid addition. Hammett's function H_0 is then calculated and presented in Table 10. If $\text{p}K(\text{HI})_{\text{s}}$ in the PIL is supposed to have the same value as in an aqueous environment: $\text{p}K(\text{HI})_{\text{s}} = \text{p}K(\text{HI})_{\text{aq}} = 7.0$, plotting $\log[(A_{\text{max}} - A)/(A - A_{\text{min}})]$ vs $\log[\text{CH}_3\text{COOH}]_{\text{aj}}$, a line with a slope of 1 and the y-intercept b corresponds to $b = \text{p}K(\text{HI})_{\text{s}} - \text{p}K_{\text{a}}(\text{CH}_3\text{COOH})_{\text{s}} - \log[\text{CH}_3\text{COO}^-]$, as shown in Figure 12. We get then $\text{p}K_{\text{a}}(\text{CH}_3\text{COOH})_{\text{s}} = 6.6$ so the acetic acid seems weaker in a $[\text{Pyr}][\text{CH}_3\text{COO}]$ environment than in aqueous environment where $\text{p}K_{\text{a}}(\text{CH}_3\text{COOH})_{\text{aq}} = 4.7$. Moreover, observing the Hammett's constants H_0 for $[\text{H}^+] = 480 \text{ mmol L}^{-1}$ shows that the $[\text{Pyr}][\text{CH}_3\text{COO}]$ is a neutral environment ($H_0 = 8.04$) compared with $[\text{BMIM}][\text{HNTf}_2]$ for $[\text{H}^+] = 337 \text{ mmol L}^{-1}$ ($H_0 = -5.05$).⁵⁵ This result confirms the pH value measured for the PIL (Table 10) $\text{pH}([\text{Pyr}][\text{CH}_3\text{COO}]) = 7.7$.

4. Conclusion

The six pyrrolidinium-based Brønsted acid PILs examined here were prepared by a simple atom-economic neutralization reaction. The density, viscosity, conductivity, electrochemical window, phase behavior and acidity scale were measured and investigated in detail. The resulting physical properties show

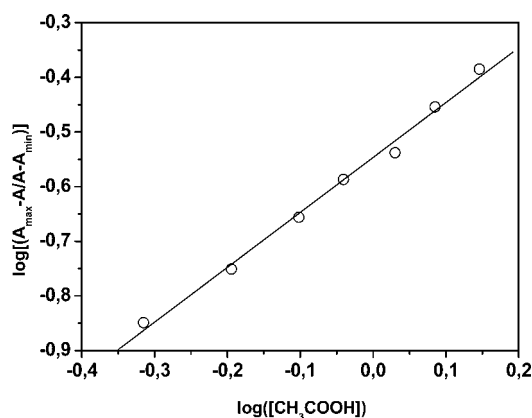


Figure 12. Variation of the Hammett functions H_0 for various concentrations of added acetic acid in $[\text{pyr}][\text{CH}_3\text{COO}]$.

that the effect of anion identity is preponderant. As a result, simple variations in anion structure or, overall, ionic composition illustrate the ease with which physical properties of a class of PILs can be modified to produce a wide range of solvents. The characterization of this PILs show that pyrrolidinium-based PILs are good (or superionic) and very fragile liquids. These PILs could be produced easily in large amounts and have potentially wide applicable perspectives for fuel cell electrolytes, and acid-catalyzed reaction environments or catalysts as replacements for conventional inorganic acids.

References and Notes

- (1) McEwen, A. B.; Ngo, H. L.; LeCompte, K.; Goldman, J. L. *J. Electrochem. Soc.* **1999**, *146*, 1687.
- (2) Shobukawa, H.; Tokuda, H.; Susan, A. B. H.; Watanabe, M. *Electrochim. Acta* **2005**, *50*, 3872.
- (3) Wang, P.; Zakeeruddin, S. M.; Shaik, M.; Humphry-Baker, R.; Grätzel, M. *Chem. Mater.* **2004**, *16*, 2694.
- (4) Brazier, A.; Appetecchi, G. B.; Passerini, S.; Surca Vuk, A.; Orel, B.; Donsanti, F.; Decker, F. *Electrochim. Acta* **2007**, *52*, 4792.
- (5) Egashira, M.; Okada, S.; Yamaki, J.; Dri, D. A.; Bonadies, F.; Scrosati, B. *J. Power Sources* **2004**, *138*, 240.
- (6) Bonhôte, P.; Dias, A. P.; Papageorgiou, N.; Kalyanasundaram, K.; Grätzel, M. *Inorg. Chem.* **1996**, *35*, 1168.
- (7) Forsyth, S.; Golding, J.; MacFarlane, D. R.; Forsyth, M. *Electrochim. Acta* **2001**, *46*, 1753.
- (8) Dere, R. T.; Pal, R. R.; Patil, P. S.; Salunkhe, M. M. *Tetrahedron Lett.* **2003**, *44*, 5351.
- (9) Karpinski, Z. J.; Osteryoung, R. A. *Inorg. Chem.* **1984**, *23*, 1491.
- (10) Krossing, I.; Slattery, J. M.; Dagueuet, C.; Dyson, P. J.; Oleinikova, A.; Weingärtner, H. *J. Am. Chem. Soc.* **2006**, *128*, 13427.
- (11) Wilkes, J. S. *Green Chem.* **2002**, *4*, 73.
- (12) Welton, T. *Chem. Rev.* **1999**, *99*, 2071.
- (13) Dupont, J.; de Souza, R. F.; Suarez, P. A. *Chem. Rev.* **2002**, *102*, 3667.
- (14) Earle, M. J.; Seddon, K. R. *Pure Appl. Chem.* **2000**, *72*, 1391.
- (15) Wasserscheid, P.; Keim, W. *Angew. Chem.* **2000**, *112*, 3926.
- (16) Holbrey, J. D.; Seddon, K. R. *Clean Prod. Process.* **1999**, *1*, 223.
- (17) Heintz, A. *J. Chem. Thermodyn.* **2005**, *37*, 525.
- (18) Ngo, H. L.; LeCompte, K.; Hargens, L.; McEwen, A. B. *Thermochem. Acta* **2000**, *357*, 97.
- (19) Ogihara, W.; Sun, J.; Forsyth, M.; MacFarlane, D. R.; Yoshizawa, M.; Ohno, H. *Electrochim. Acta* **2004**, *49*, 1797.
- (20) Nakagawa, H.; Izuchi, S.; Kuwana, K.; Nukuda, T.; Aihara, Y. *J. Electrochem. Soc.* **2003**, *150*, 695.
- (21) Doyle, M.; Choi, S.; Proulx, G. *J. Electrochem. Soc.* **2000**, *147*, 34.
- (22) Gordon, C. *Appl. Catal. A: Gen.* **2001**, *222*, 101.
- (23) Olivier-Bourbigou, H.; Magna, L. *J. Mol. Catal. A: Chem.* **2002**, *182–183*, 419.
- (24) Sheldon, K. R. *Chem. Commun.* **2001**, 2399.
- (25) Susan, M. A. H.; Noda, A.; Mitsushima, S.; Watanabe, M. *Chem. Commun.* **2003**, 938.
- (26) Lewandowski, A.; Swiderska, A. *Solid State Ionics* **2003**, *161–243*.
- (27) (a) Harris, K. R.; Kanakubo, M.; Woolf, L. A. *J. Chem. Eng. Data* **2007**, *52* (3), 1080. (b) Tokuda, H.; Tsuzuki, S.; Susan, M. A. B. H.; Hayamizu, K.; Watanabe, M. *J. Phys. Chem. B* **2006**, *110*, 19593. (c) Sanmamed, Y. A.; Gonzalez-Salagado, D.; Troncoso, J.; Cerdeirina, C. A.; Romani, L. *Fluid Phase Equilib.* **2007**, *252*, 96. (d) Pereira, A. B.; Legido, J. L.; Rodriguez, A. *J. Chem. Thermodyn.* **2007**, *39*, 1168.
- (28) Greaves, L. T.; Drummond, C. J. *Chem. Rev.* **2008**, *108*, 206.
- (29) Okoturo, T. J.; VanderNoot, J. *Electroanal. Chem.* **2004**, *568*, 167.
- (30) MacFarlane, D. R.; Sun, J.; Golding, J.; Meakin, P.; Forsyth, M. *Electrochem. Commun.* **2000**, *45*, 1271.
- (31) Tao, G. H.; He, L.; Sun, N.; Kou, Y. *Chem. Commun.* **2005**, 3562.
- (32) Galinski, M.; Lewandowski, A.; Stepniak, I. *Electrochim. Acta* **2006**, *51*, 5567.
- (33) Greaves, T. L.; Weerawardena, A.; Fong, C.; Krodziewska, I.; Drummond, C. J. *J. Phys. Chem. B* **2006**, *110*, 22479.
- (34) Reichardt, C. *Green Chem.* **2005**, *7*, 339.
- (35) MacFarlane, D. R.; Pringle, J. M.; Johansson, K. M.; Forsyth, S. A.; Forsyth, M. *Chem. Commun.* **2006**, 1905.
- (36) Maruyama, T.; Nagasawa, S.; Goto, M. *Biotechnol. Lett.* **2002**, *24*, 1341.
- (37) MacFarlane, D. R.; Meakin, P.; Sun, J.; Amini, N.; Forsyth, M. *J. Phys. Chem. B* **1999**, *103*, 4164.
- (38) Noda, A.; Watanabe, M. *Electrochim. Acta* **2000**, *45*, 1265.

- (39) Andrieux, C. P.; Gonzalez, F.; Savéant, J.-M. *J. Electroanal. Chem.* **2001**, 498, 171–180.
- (40) Van Valkenburg, M. E.; Vaughn, R. L.; Williams, M.; Wilkes, J. S. *Thermochim. Acta* **2005**, 425–181.
- (41) Wilkes, J. S. *J. Mol. Catal. A: Chem.* **2004**, 214, 11.
- (42) Walden, P. Z. *Phys. Chem.* **1906**, 55207 a, nd 246.
- (43) Bockris, J. O. M.; Reddy, A. K. N. *Modern Electrochemistry*, 2nd ed. Plenum Press: New York, 1998.
- (44) Matsumoto, H.; Yanagida, M.; Tanimoto, K.; Nomura, M.; Kitagawa, Y.; Miyazaki, Y. *Chem. Lett.* **2000**, 29–922.
- (45) Forsyth, S.; Golding, J.; MacFarlane, D. R.; Forsyth, M. *Electrochim. Acta* **2001**, 46–1753.
- (46) Xu, W.; Cooper, E. I.; Angell, C. A. *J. Phys. Chem. B* **2003**, 107, 6170.
- (47) D Ediger, M.; Angell, C. A.; Nagel, S. R. *J. Phys. Chem.* **1996**, 100, 13200.
- (48) Angell, C. A.; MacFarlane, D. R.; Oguni, M. *Ann. N. Y. Acad. Sci.* **1986**, 484–241.
- (49) Angell, C. A. *J. Phys. Chem. Solids* **1988**, 49–863.
- (50) Donth, E. *J. Non-Cryst. Solids* **1982**, 53–325.
- (51) Hodge, I. M. *J. Non-Cryst. Solids* **1996**, 202–164.
- (52) Richert, R.; Angell, C. A. *J. Chem. Phys.* **1998**, 108–9016.
- (53) Belieres, J.-P.; Angell, C. A. *J. Phys. Chem. B* **2007**, 111–4926.
- (54) Duan, Z.; Gu, Y.; Zhang, J.; Zhu, L.; Deng, Y. *J. Mol. Catal. A: Chem.* **2006**, 250, 163.
- (55) Thomazeau, H.; Olivier-Bourbigou, L.; Luts Magna, S.; Gilbert, B. *J. Am. Chem. Soc.* **2003**, 125, 5264.

JP805992B